Langmuir
Article
pubs.acs.org/Langmuir

Interaction of Carbon Monoxide with Au(111) Modified by Ion Bombardment: A Surface Spectroscopy Study under Elevated Pressure†

Zoltán Pászti,[‡] Orsolya Hakkel,[‡] Tamás Keszthelyi,[‡] András Berkó,[‡,§] Nándor Balázs,[‡] Imre Bakó,[‡] and László Guczi*[,‡,∥]

[‡]*Chemical Research Center, Hungarian Academy of Sciences, P.O. Box 17, H-1525 Budapest, Hungary,* [§]*University of Szeged, Department of Physical Chemistry and Material Science, P.O. Box 168, H-6701 Szeged, Hungary, and* [∥]*Institute of Isotopes, Hungarian Academy of Sciences, P.O. Box 77, H-1525 Budapest, Hungary*

Received April 15, 2010. Revised Manuscript Received May 28, 2010

Gold based model systems exhibiting the structural versatility of nanoparticle ensembles and being accessible for surface spectroscopic investigations are expected to provide new information about the adsorption of carbon monoxide, a key process influencing the CO oxidation activity of this noble metal in nanoparticulate form. Accordingly, in the present work the interaction of CO is studied with an ion bombardment modified Au(111) surface by means of a combination of photoelectron spectroscopy (XPS and UPS), sum frequency generation vibrational spectroscopy (SFG), and scanning tunneling microscopy (STM). While no adsorption was found on intact Au(111), data collected on the ion bombarded surface at cryogenic temperatures indicated the presence of stable CO adsorbates below 190 K. A quantitative evaluation of the C 1s XPS spectra and the surface morphology explored by STM revealed that the step edge sites created by ion bombardment are responsible for CO adsorption. The identification of the CO binding sites was confirmed by density functional theory (DFT) calculations. Annealing experiments up to room temperature showed that at temperatures above 190 K unstable adsorbates are formed on the surface under dynamic exposure conditions that disappeared immediately when gaseous CO was removed from the system. Spectroscopic data as well as STM records revealed that prolonged CO exposure at higher pressures of up to 1 mbar around room temperature facilitates massive atomic movements on the roughened surface, leading to its strong reordering toward the structure of the intact Au(111) surface, accompanied by the loss of the CO binding capacity.

Introduction

Since the discovery of the catalytic activity of oxide-supported gold nanoparticles by Haruta et al.,[1,2] a vast amount of information was collected on the strikingly reactive behavior of this noble metal when in nanosized form. Because gold is one of the chemically most inert transition metals, it is still puzzling why gold nanoparticles at a size of 2−4 nm supported on oxides with variable oxidation states (TiO_2, Fe_2O_3, and Co_2O_3) have very high activity in CO oxidation.[3] Although CO oxidation is unquestionably the most widely investigated process catalyzed by gold,[2,4,5] supported gold catalysts turned out to be active in a series of reactions important in the production of fine chemicals such as alkene epoxidation[2,6] or the oxidation of glucose[7] and alcohols.[8] Apart from oxidation processes, gold also seems to be a useful catalyst in hydrogenation reactions,[8] including those with unsaturated hydrocarbons[2] or even oxygen to form hydrogen peroxide.[9] Gold also catalyzes the alcohol reforming process.[10] In a model study, even CO_2 turned out to disproportionate over potassium-promoted Au(111).[11]

In spite of the impressive range of catalytic investigations, several fundamental aspects of gold catalysis are still not completely understood.[12] For example, as far as the nature of the active site in carbon monoxide oxidation over transition metal oxide-supported gold catalysts is concerned, there are at least three different theories proposed: all important reaction steps may occur on the Au nanoparticle surface, and the oxide support remains passive throughout the process;[13,14] oxygen activation may take place at oxygen vacancies in the support whereas O spillover can oxidize the CO adsorbates bound to gold nanoparticles,[15] which could locate the active site at the nanoparticle-support perimeter;[16,17] or the interaction of molecular oxygen with CO may lead to the formation of gold carbonate, which can transform to CO_2 upon reaction with another CO molecule.[18]

Investigations on well-defined model systems under carefully controlled conditions are expected to give significant guidance in

† Part of the Molecular Surface Chemistry and Its Applications special issue.

*Corresponding author. Fax: +36-1-392-2703. E-mail: guczi@mail.kfki.hu.

(1) Haruta, M. *Catal. Today* **1997**, *36*, 153–166.
(2) Haruta, M.; Date, M. *Appl. Catal., A* **2001**, *222*, 427–437.
(3) Herzing, A. A.; Kiely, J. C.; Carley, A. F.; Landon, P.; Hutchings, G. J. *Science* **2008**, *321*, 1331–1335.
(4) Hutchings, G. J.; Brust, M.; Schmidbaur, H. *Chem. Soc. Rev.* **2008**, *37*, 1759–1765.
(5) Hashmi, A. S. K.; Hutchings, G. J. *Angew. Chem.* **2006**, *45*, 7896–7936.
(6) Hughes, M. D.; Xu, Y.-J.; Jenkins, P.; McMorn, P.; Landon, P.; Enache, D. I.; Carley, A. F.; Attard, G. A.; Hutchings, G. J.; King, F; Stitt, E. H.; Johnston, P.; Griffin, K.; Kiely, C. J. *Nature* **2005**, *347*, 1132–35.
(7) Dimitratos, N.; Lopez-Sanchez, J. A.; Hutchings, G. J. *Top. Catal.* **2009**, *52*, 258–268.
(8) Hutchings, G. J. *Catal. Today* **2007**, *122*, 196–200.
(9) Hutchings, G. J. *J. Mater. Chem.* **2009**, *19*, 1222–1235.
(10) Gazsi, A.; Bánsági, T.; Solymosi, F. *Catal. Lett.* **2009**, *131*, 33–41.
(11) Farkas, A. P.; Solymosi, F. *J. Phys. Chem. C* **2009**, *113*, 19930–19936.
(12) Lopez, N.; Janssens, T. V. W.; Clausen, B. S.; Xu, Y.; Mavrikakis, M.; Bligaard, T.; Nørskov, J. K. *J. Catal.* **2004**, *223*, 232–235.
(13) Schubert, M. M.; Hackenberg, S.; van Veen, A. C.; Muhler, M.; Plzak, V.; Behm, J. *J. Catal.* **2001**, *197*, 113.
(14) Deng, X.; Min, B. K.; Guloy, A.; Friend, C. M. *J. Am. Chem. Soc.* **2005**, *127*, 9267–9270.
(15) Grunwaldt, J. D.; Baiker, A. *J. Phys. Chem. B* **1999**, *103*, 1002–1012.
(16) Guczi, L.; Peto, G.; Beck, A.; Frey, K.; Geszti, O.; Molnár, G.; Daróczi, Cs. *J. Am. Chem. Soc.* **2003**, *125*, 4332–4337.
(17) Guczi, L.; Frey, K.; Beck, A.; Peto, G.; Daróczi, Cs.; Kruse, N.; Chenakin, S. *Appl. Catal., A* **2005**, *291*, 116–125.
(18) Hakkinen, H; Landman, U. *J. Am. Chem. Soc.* **2001**, *123*, 9704.

clarifying these controversial issues by providing new insights into the processes occurring on the surfaces of gold catalysts. The instrumentation and methodology of traditional ultrahigh vacuum based surface science provides a solid starting point for this approach. Nevertheless, there is still a rather limited number of studies dealing with gas adsorption and/or simple reactions on gold single crystals[19] that can be regarded as the simplest form of well-defined models of catalytically active gold.

Gold surfaces are in general rather inactive toward dissociation or even the adsorption of small probe molecules such as oxygen, hydrogen, and carbon monoxide.[19] Oxygen adsorbates were observed on single-crystalline Au surfaces only after treatment with atomic oxygen.[14,20] Interestingly, preadsorbed oxygen enhances both oxygen dissociation[14] and CO oxidation[21] over Au(111), suggesting that the presence of atomic oxygen on the surface may be a crucial factor in oxidative processes catalyzed by gold.[22] Although carbon monoxide is generally believed not to interact with Au(111), it adsorbs to some extent on more open surfaces such as (110).[23,24] Experiments performed under low temperature/low pressure conditions on stepped Au single crystal surfaces revealed their relatively stronger interaction with CO,[25−27] in excellent agreement with computational predictions[28] emphasizing the role of coordinatively unsaturated gold sites.[12]

On comparison of these results with data concerning real gold catalysts, one has to keep in mind that an ensemble of oxide-supported Au nanoparticles has a much wider range of structural elements (crystal faces, steps, terraces, edges, and kinks and their location with respect to the support) than that one could prepare on a single crystal face of any orientation. Obviously, this issue can be dealt with by developing model systems of increasing structural complexity, for example, by comparing data measured on single crystals, textured and nontextured thin films on appropriate substrates,[15] or different forms of supported Au nanostructures.[29] Another possibility is to modify an originally smooth single crystal surface by low energy ion bombardment, which is known to generate structural alterations ranging from adatoms/vacancies[30−32] to hills and valleys on the micrometer scale,[33,34] depending on the parameters of ion exposure. Indeed, CO adsorption experiments reveal significantly different behavior when intact and ion bombarded gold faces are compared. TPD traces, along with infrared absorption spectra, STM images, and computational studies suggest tentatively that similar to the vicinal (111) surfaces,[27] the step atoms are responsible for the binding of CO[35,36] on the ion-bombarded modified surface.

Apart from issues related to structural complexity, separate efforts are required to reduce the difference in the working conditions (e.g., pressure, temperature, and gas composition) of practical catalysts and well-controlled model systems, which, according to the prerequisites of the surface science methodology, are typically investigated at low pressure (often in ultrahigh vacuum) and low temperature. As a result, recent trends in surface science imply the emergence of in situ or even operando investigation techniques[37] such as optical spectroscopic methods, which seem to provide particularly useful information about the adsorption and transformation of gaseous species. Sum frequency generation vibrational spectroscopy (SFG), a spectroscopic tool based on a second-order nonlinear optical effect, offers unique and excellent opportunities for the molecular level investigation of surface chemical processes under realistic conditions. As the result of its inherent surface specificity and submonolayer sensitivity, the method is capable of studying interfacial phenomena at gas−solid, liquid−solid, and even liquid−liquid interfaces.[38−41]

In our laboratory, a novel experimental setup was developed by connecting an SFG spectrometer to a multitechnique surface analysis system via a dedicated chamber designed for experiments at elevated pressures over a broad temperature range.[42] This complex instrument allows for sample preparation and characterization according to the standards of traditional surface science as well as the in situ determination of the gas adsorption and transformation properties of the sample at ambient pressure. In the setup, the sample is not exposed to air during preparation, characterization, and SFG measurement, thus its surface composition and electronic structure can be unambiguously related to its gas adsorption properties.

In this study, our aim is to characterize the interaction of carbon monoxide with ion bombardment modified gold surfaces at low temperatures and pressures as well as at conditions more closely resembling the working range of real CO oxidation catalysts. Au(111) was chosen as the starting surface, mostly driven by the fact that supported Au nanoparticles exhibit predominantly (111) faces because of surface energy reasons, along with a much smaller number of other low index faces.[43] Considering the versatility of the morphological elements created by sputtering, we believe that an ion bombardment roughened (111) surface represents a better approximation to the structural complexity of a nanoparticle ensemble than any intact single crystal face.

First, we present our data on the CO adsorption properties of ion bombarded Au(111) at low temperature. These results, together with information available in the literature, validate our methodology and establish the starting point for the interpretation of the adsorption behavior of CO at intermediate (just above the CO desorption temperature in UHV) and higher temperatures, for which, to our knowledge, a systematic surface spectroscopy study was not performed. Information about vibrational

(19) Carabineiro, S. A. C.; Nieuwenhuys, B. E. *Gold Bull.* **2009**, *42*, 288–300.
(20) Kim, J.; Samano, E.; Koel, B. E. *Surf. Sci.* **2006**, *600*, 4622–4632.
(21) Min, B. K.; Alemozafar, A. R.; Pinnaduwage, D.; Deng, X.; Friend, C. M. *J. Phys. Chem. B* **2006**, *110*, 19833–19838.
(22) Wittstock, A.; Zielasek, V.; Biener, J.; Friend, C. M.; Bäumer, M. *Science* **2010**, *327*, 319–322.
(23) Gottfried, J. M.; Schmidt, K. J.; Schroeder, S. L. M.; Christmann, K. *Surf. Sci.* **2003**, *536*, 206–224.
(24) Sandell, A.; Bennich, P.; Nilsson, A.; Hernnäs, B.; Björneholm, O.; Mårtensson, N. *Surf. Sci.* **1994**, *310*, 16–26.
(25) Ruggiero, C.; Hollins, P. *Surf. Sci.* **1997**, *377−379*, 583–586.
(26) Kim, J.; Samano, E.; Koel, B. E. *J. Phys. Chem. B* **2006**, *110*, 17512–17517.
(27) Weststrate, C. J.; Lundgren, E.; Andersen, J. E.; Rienks, E. D. L.; Gluhoi, A. C.; Bakker, J. W.; Groot, I. M. N.; Nieuwenhuys, B. E. *Surf. Sci.* **2009**, *603*, 2152–2157.
(28) Mavrikakis, M.; Stoltze, P.; Nørskov, J. K. *Catal. Lett.* **2000**, *64*, 101–106.
(29) Lemire, C.; Meyer, R.; Shaikhutdinov, Sh.K.; Freund, H.-J. *Surf. Sci.* **2004**, *552*, 27–34.
(30) Michely, T.; Comsa, G. *Phys. Rev. B* **1991**, *44*, 8411–8414.
(31) Naumann, J.; Osing, J.; Quinn, A. J.; Shvets, I. V. *Surf. Sci.* **1997**, *388*, 212–219.
(32) Chan, W. L.; Chason, E. *J. Appl. Phys.* **2007**, *101*, 121301.
(33) Carter, G.; Colligon, J. S.; Nobes, M. J. *Radiation Effects* **1977**, *31*, 65–87.
(34) Auciello, O. *J. Vac. Sci. Technol.* **1981**, *19*, 841–867.
(35) Yim, W.-L.; Nowitzki, T.; Necke, M.; Schnars, H.; Nickut, P.; Biener, J.; Biener, M. M.; Zielasek, V.; Al-Shamery, K.; Bäumer, M. *J. Phys. Chem. C* **2007**, *111*, 445–451.
(36) Biener, J.; Biener, M. M.; Nowitzki, T.; Hamza, A. V.; Friend, C. M.; Zielasek, V.; Bäumer, M. *ChemPhysChem* **2006**, *7*, 1906–1908.
(37) Rupprechter, G. *Catal. Today* **2007**, *126*, 3–17.
(38) Yang, M. C.; Chou, K. C.; Somorjai, G. A. *J. Phys. Chem. B* **2004**, *108*, 14766–14779.
(39) Chen, Z.; Shen, Y.-R.; Somorjai, G. A. *Annu. Rev. Phys. Chem.* **2002**, *53*, 437–465.
(40) Richmond, G. L. *Annu. Rev. Phys. Chem.* **2001**, *52*, 357–389.
(41) Clarke, M. L.; Wang, J.; Chen, Z. *J. Phys. Chem. B.* **2005**, *109*, 22027–22035.
(42) Hakkel, O.; Pászti, Z.; Keszthelyi, T.; Guczi, L. *React. Kinet. Catal. Lett.* **2009**, *96*, 345–356.
(43) Marks, L. D. *Rep. Prog. Phys.* **1994**, *57*, 603.

and electronic features of the CO/Au systems will be analyzed in terms of structural data from scanning tunneling microscopy measurements and density functional theory calculations.

Experimental Section

Materials. The Au(111) single crystal (orientation accuracy within 1°) was purchased from MaTeck GmbH (Germany) and was cleaned in the surface analysis system by repeated cycles of 2 to 3 keV Ar^+ sputtering and annealing to 900 K until no contaminants were detected by XPS and the characteristic UPS spectrum of Au(111)[44] was obtained. Scanning tunneling microscopy measurements carried out in a separate instrument confirmed the herringbone reconstruction of the surface after this treatment.

Carbon monoxide (purity 4.7) was purchased from Linde Hungary in an aluminum cylinder in order to reduce the contamination from transition metal (mostly Ni) carbonyls. The gas was used without further purification.

Surface Analysis System. The experimental work has been carried out in a system based on a sum frequency spectrometer made by EKSPLA (Vilnius, Lithuania). The visible beam (532 nm) used for the SFG studies is generated by doubling the fundamental output of a Nd:YAG laser (1064 nm wavelength, 20 ps pulse width, 20 Hz repetition rate) in a harmonics unit. The tunable IR beam is obtained from an optical parametric generation/difference frequency generation system. The beam energies at the sample vary from 10 to 250 μJ with a spot size of 0.2 mm × 1 mm. Sum frequency light is collected in the reflected direction through a holographic notch filter and monochromator and detected by a photomultiplier. The spectral resolution is determined by the ~6 cm^{-1} line width of the IR pulse. The spectrometer is completed with two sample stages: one exposed to atmospheric conditions and one housed in the UHV-high pressure cell of the surface analytical system.

The surface analytical system manufactured by OMICRON Nanotechnology GmbH (Germany) consists of three chambers. The analytical chamber is equipped with an electron beam evaporation source and a fine focus ion gun for sample preparation, an EA 125-type hemispherical energy analyzer, a dual-anode X-ray source, and a differentially pumped gas discharge lamp for X-ray and ultraviolet photoelectron spectroscopy. Two turbomolecular pumps, an ion pump, and a titanium sublimation pump provide a base pressure of around 1×10^{-10} to 2×10^{-10} mbar with mostly hydrogen as the residual gas. The vital part of the system is the dedicated SFG chamber in which experiments can be performed from ultrahigh vacuum (better than 5×10^{-9} mbar) to atmospheric pressure. Fast evacuation of the SFG chamber is ensured by a separate turbopump. Laser beams necessary for SFG measurements are introduced into the chamber via large CaF_2 windows. The chamber is equipped with a gas manifold and a Pfeiffer (Germany)-made PRISMA mass spectrometer. Further sample preparation tools can be attached to the preparation chamber. Fast, precise sample handling is facilitated by a loadlock system and two manipulators.

Sample temperatures can be measured by K-type thermocouples attached to the standard Omicron sample holder. The sample temperature in the analysis chamber can be lowered to 120 K by liquid nitrogen cooling and elevated to 1100 K by resistive heating. Because of construction reasons, the temperature range of the manipulator in the SFG chamber is somewhat narrower and varies between 150 and 900 K.

Surface Spectroscopy Measurements. A measurment cycle always started with a short cleaning of the Au(111) single crystal and checking its status with a UPS and/or XPS measurement. Ion bombardment modified samples were prepared by 10 min of 3 keV Ar^+ etching of the single crystal surface either at room temperature or after cooling to 120 K. The angle of incidence of the Ar^+ ions was 45°, and the ion gun delivered a current density of 10 $\mu A/cm^2$. For SFG measurements, the sample was transferred immediately after roughening to the previously cooled manipulator of the SFG chamber. Gas adsorption experiments in the SFG chamber were performed in a CO flow of up to 10^{-4} mbar; pressures up to 1 mbar were achieved by backfilling the chamber with CO.

Because during a sum frequency experiment the sample is exposed to intense laser beams, special care must be exercised to avoid damage to or uncontrolled heating of the surface. We found that limiting the visible and infrared excitation energies to below 20 μJ was necessary to prevent CO desorption, even if the sample itself was able to withstand much higher beam energies without noticeable damage.

In situ electron spectroscopy measurements were carried out in the analysis chamber under CO partial pressures ranging from 10^{-9} to 10^{-5} mbar under gas flow; He lines (He I, 21.2 eV; He II, 40.8 eV) and Al Kα radiation were used for excitation. Photoelectrons were analyzed in the fixed analyzer transmission mode of the analyzer, with a 5 eV pass energy for UPS (resolution of around 100 meV) and 30 eV for XPS, which resulted in an acceptable trade-off between resolution (around 1 eV) and sensitivity. Spectra were taken in low-magnification mode, which ensured a solid angle of 1° for electron collection, providing good angular resolution for the UPS experiments. Results of the XPS measurements were processed using the CasaXPS software.[45]

Scanning Tunneling Microscopy. Structural characterization of the samples was carried out using a room temperature STM instrument (WA Technology, U.K.) installed in an UHV system equipped with ion bombardment sample cleaning, heating, gas dosing, and Auger electron spectroscopy facilities. The sample was cleaned and roughened in the same way as in the Omicron surface analysis system; Auger electron spectroscopy was used to check its cleanliness.

The STM images were recorded in constant current mode with an electrochemically etched W tip. The $X-Y-Z$ calibration of the STM head was performed by measuring the characteristic morphological parameters of the TiO_2(110)-(1 × 1) support (lateral unit cell, 2.96 × 6.50 nm; height of [001] oriented step, 2.97 nm). Special, careful tip conditioning was applied in the course of the measurements in order to obtain good atomic resolution. This contained not only course and fine bias-pulse treatments but also extended in situ annealing of the tip end at 180 V and 100 nA in feedback mode for 10−20 min. From the point of view of the present work, it is important to remark that image-processing software (SPIP) developed by Image Metrology (Denmark) was applied for the automatic identification of step lines and in this way to determine the surface concentration of the step atoms on the different gold surfaces. STM images were collected at 1 V with 10 nA tunneling current.

Theoretical Calculations

Adsorption energies and electronic and vibrational properties of CO adsorbates were calculated using the Vienna Ab Initio Simulation Package (VASP),[46] which is a density functional theory (DFT) code with a plane wave basis set. Electron−ion interactions were described using the projector-augmented wave (PAW)[47,48] method, which was expanded within a plane wave basis set up to a cutoff energy of 400 eV. Electron exchange and correlation effects were described by the Perdew−Burke−Ernzerhof (PBE)[49] GGA-type exchange−correlation functional using the spin-restricted formalism. The total energy of Au had a minimum at a 4.18 Å lattice constant, which is close to the

(44) Zimmer, H.-G.; Goldmann, A.; Courths, R. *Surf. Sci.* **1986**, *176*, 115–124.

(45) Fairley, N. www.casaxps.com.
(46) Kresse, G.; Hafner, J. *Phys. Rev. B* **1993**, *47*, C558.
(47) Kresse, G.; Furthmuller, J. *Comput. Mater. Sci.* **1996**, *6*, 15.
(48) Blöchl, P. *Phys. Rev. B* **1994**, *50*, 17953.
(49) Perdew, J. P.; Burke, K.; Ernzerhof, M. *Phys. Rev. Lett.* **1996**, *77*, 3865.

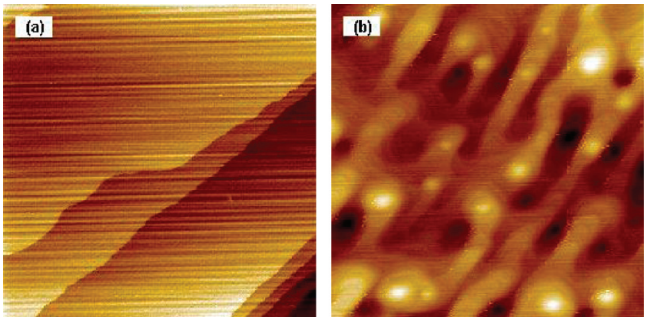

Figure 1. STM images (200×200 nm^2) recorded on (a) the intact Au(111) surface and (b) the Ar^+ sputtering modified Au(111) surface (10 min, 3 keV). Both sputtering and imaging were completed at room temperature. The z scale can be derived from the corrugation (height difference between the highest and lowest point of the imaged surface corresponding to the brightest and darkest spots), which was 1.1 nm in image (a) and 7.0 nm in image (b).

experimental value (4.08 Å). This lattice constant was used for all calculations.

Geometry optimizations were performed on a supercell structure using periodic boundary conditions. The (111) surface was modeled by three layers of metal separated by a vacuum layer of approximately 15 Å. We used a supercell with a $(3 \times 2\sqrt{3})$ surface cell to study the low coverage adsorption (surface coverage is $^1/_{12}$ ML and $^1/_3$ ML) and to investigate the CO adsorption on an adatom. The Au steps were modeled on the same unit cell with a terrace one atom deep and built up from three atom arranged in a triangle. We additionally calculated the adsorption energy of CO if we put an additional Au atom into the triangle. The two uppermost substrate layers and the CO molecules were allowed to relax, and the bottom layer of Au atoms was held fixed in their bulk position. Further details of the calculation were the same as described in our previous work.[50]

Results and Discussion

Adsorption of CO on Au(111) Modified by Ion Bombardment at Low Temperature. Prior to analyzing the adsorption behavior of carbon monoxide on ion bombarded Au(111), we tested its interaction with the intact surface. In accordance with the vast majority of the corresponding literature,[19] our data confirmed that carbon monoxide does not adsorb in a measurable quantity even at elevated pressures of up to 1 mbar. Further details about these investigations are presented as Supporting Information.

Temperature programmed desorption experiments on Au(110)[24] or vicinal (111)[25−27] surfaces as well as ion bombardment modified samples[35,36] indicated that a saturated CO layer desorbs below 190 K. In the present subsection, we will summarize our findings on the interaction of CO with the ion bombarded Au(111) surface below this temperature. Effects of annealing to higher temperatures will be discussed separately.

Morphology of the Sputter Modified Au(111) Surface. In Figure 1, scanning tunneling images of the intact and ion bombardment modified Au(111) surface are shown. The intact surface is characterized by large, atomically smooth terraces, with monatomic steps between the terraces. The corrugation (height difference between the highest and lowest points of the imaged surface) was 1.1 nm. To facilitate comparison with results obtained on the ion bombardment modified surfaces, a statistical analysis of the density of Au atoms belonging to step edge sites was performed by the SPIP software mentioned in the Experimental Section. According to this analysis, the concentration of step edge atoms on the intact Au(111) surface was around $6(\pm 0.9) \times 10^{12}$ /cm^2. For reference, the atomic density of the nonreconstructed Au(111) surface calculated from bulk parameters is 1.4×10^{15} /cm^2.

Ion bombardment removed the large, flat terraces; instead, pitlike and moundlike structures were created, with holes as deep as six to eight atomic layers and protrusions of nearly the same height, which is reflected in the increased corrugation value (7.0 nm). In fact, the protrusions can be regarded in some sense as gold-supported gold nanoparticles. The STM images reveal that ion bombardment increased the density of steps significantly whereas the typical terrace width was considerably reduced, especially at the side walls of the pits and mounds. Interestingly, although ion bombardment transformed the surface into a 3D structure, the dominant morphological elements are still (111) terraces. According to the quantitative analysis of several images taken on freshly sputtered surfaces, sputtering increased the density of Au atoms located at step edge sites by almost 2 orders of magnitude to $2.4(\pm 0.3) \times 10^{14}$ step atoms/cm^2. The morphology is qualitatively similar to that observed in ref 35 or 51 under tentatively similar preparation conditions. In fact, this morphology can be regarded as typical of room temperature sputtered fcc metal surfaces; mechanisms leading to its formation are discussed in the literature.[31,32]

CO Adsorption on Sputter Modified Au(111) below 190 K. A combination of surface sensitive spectroscopic methods including UPS, XPS, and SFG was applied to study the adsorption behavior of CO on ion bombarded Au(111). Before presenting the results, it is worth analyzing the valence band UPS spectra of the intact as well as the sputtered Au surfaces, to which data measured after CO exposure will be related.

Normal emission spectra of the unsputtered Au(111) surface excited by He I and He II radiation are shown in Figure 2a,b (lowermost traces). The spectra are identical to those found in the literature for Au(111) surfaces.[44] The assignment of the various spectral features is well-established. The narrow peak at around 0.45 eV binding energy is due to the Shockley surface state,[44,52,53] which is localized in the first few atomic layers[54] and, as demonstrated in the Supporting Information, is structure-sensitive.[53] In addition, this state interacts with adsorbates; therefore, it can be used as a sensitive probe for adsorption processes.[55−57] The features between 2 and 7 eV arise from the d band. The peaks at 3.7, 4.7, and 6.0 eV binding energy are due to direct transitions from bulk Au bands.[58] The small peak at 4.3 eV and the shoulder at 5.7 eV can be attributed to emission from localized surface states.[44]

In spite of the significant morphological modifications, the spectrum of the sputtered surface (Figure 2, second curve from the bottom) is still dominated by the three relatively narrow peaks of the bulk d bands. Nevertheless, the intensity ratios significantly changed; in particular, the 6.0 eV binding energy peak, which was

(50) Krenn, G.; Bakó, I.; Schennach, R. *J. Chem. Phys.* **2006**, *124*, #144703.
(51) Zielasek, V.; Xu, B.; Liu, X.; Bäumer, M.; Friend, C. M. *J. Phys. Chem. C* **2009**, *113*, 8924–8929.
(52) Shockley, W. *Phys. Rev.* **1939**, *56*, 317–323.
(53) Paniago, R.; Matzdorf, R.; Meister, G.; Goldmann, A. *Surf. Sci.* **1995**, *336*, 113–122.
(54) Mazzarello, R.; Dal Corso, A.; Tosatti, E. *Surf. Sci.* **2008**, *602*, 893–905.
(55) Nicolay, G.; Reinert, F.; Forster, F.; Ehm, D.; Schmidt, S.; Eltner, B.; Hüfner, S. *Surf. Sci.* **2003**, *543*, 47–56.
(56) Whelan, C. M.; Barnes, C. J.; Walker, C. G. H.; Brown, N. M. D. *Surf. Sci.* **1999**, *425*, 195–211.
(57) Kanai, K.; Ouchi, Y.; Seki, K. *Thin Solid Films* **2009**, *517*, 3276–3280.
(58) Courths, R.; Zimmer, H.-G.; Goldmann, A.; Saalfeld, H. *Phys. Rev. B* **1986**, *34*, 3577–3585.

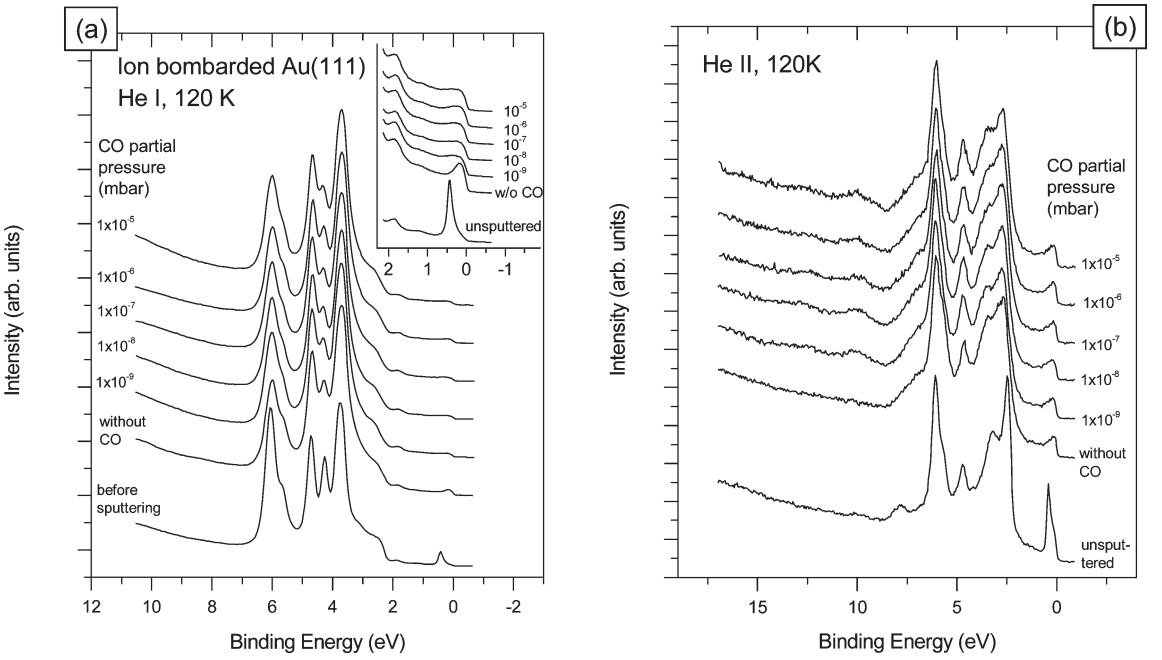

Figure 2. Valence band UPS spectra of Au(111) modified by 10 min of 3 keV Ar^+ ion bombardment measured during exposure to different partial pressures of CO. All spectra were taken in normal emission at 120 K and are shifted vertically for clarity. For reference, the spectra of the intact Au(111) surface are also included. (a) He I (21.2 eV) excitation. (Inset) Enlarged view in the vicinity of the Fermi level. (b) He II (40.8 eV) excitation.

almost as equally intense as the 3.7 eV peak in the unsputtered case, became the weakest contribution after surface modification, suggesting that this peak has a pronounced sensitivity to structural order beyond the first few neighbors.[44] In addition, the relative intensity of the surface state peak at 4.3 eV became significantly weaker. Finally, the Shockley surface state peak disappeared (see inset), and instead a relatively weak, broad feature appeared much closer to the Fermi level than the Shockley surface state. Following literature results obtained on vicinal Au(111) surfaces[59] or graphite-supported Au nanoparticles,[60] we tentatively assign this feature to 2D electron gas on (111) faces/terraces confined spatially by the morphological elements introduced by the sputter roughening. The small peak at 1.8 eV binding energy is most probably due to excitation by the He I satellite line at 23.1 eV.

UPS spectra of Figure 2 indicate that CO readily interacts with the roughened Au(111) surface. In the He II excited spectra (which are more surface specific than the He I excited ones for electron mean free path reasons), two new bands assignable to CO adsorbates appear at 10.0 and 12 to 13 eV binding energies. The structure at 10.0 eV arises from the nearly degenerate CO $5\sigma-1\pi$ states, and the feature at 12.5 eV is due to the 4σ levels.[23,24] In addition, significant modifications can be seen in both surface-related states in the He I excited spectrum: the peak in the vicinity of the Fermi level disappears and the spectral intensity significantly decreases on the low binding energy side of the 4.3 eV peak of the d band. These changes suggest an electronic interaction between the CO adsorbates and certain electronic states of the sputter modified Au(111) surface: either these electrons directly participate in Au−CO bond formation or the local environment of the morphological elements responsible for these states changes during CO adsorption in such a way that it leads to their disappearance; nevertheless, a detailed discussion of such processes is beyond the scope of this article.

An inspection of the spectra in Figure 2, especially of those with signals directly related to CO adsorbates, suggests that the amount of adsorbed CO is rather low but does not change even if the CO pressure is varied by 4 orders of magnitude. A more direct estimation of the quantity of adsorbed CO can be derived from X-ray photoelectron spectroscopy measurements. Because of technical reasons, the deconvolution of the CO signals is not straightforward; details of the processing and analysis of the XPS data are given in the Supporting Information. The position (288−289 eV) and the line shape of the measured C 1s envelope obtained as a result of the deconvolution process correspond well to data measured on stepped Au(310) and (321) surfaces with CO adsorbates.[27] An order-of-magnitude-type estimation of the amount of adsorbed CO based on the C 1s and Au 4f intensities was also performed (details in Supporting Information); the results are presented in Figure 3a as a function of the applied CO partial pressure. The data show that the amount of adsorbed CO saturates at around $1.5-1.7 \times 10^{14}$ molecules/cm^2 at CO pressures above 10^{-8} mbar. Error bars were calculated from three to four independent measurements at a given pressure (in all cases on a freshly prepared surface).

As another indicator of CO adsorption, the work function of the sample was determined from UPS data by calculating the difference between the photon energy (21.2 eV) and the width of the He I excited spectrum (from the low kinetic energy cutoff to the Fermi level). The work function of the sputter-modified surface turned out to be 5.2−5.3 eV, which is essentially the same as that of intact Au(111).[61,62] In Figure 3a, data concerning the CO pressure dependent behavior of the work function on the sputter modified surface are also presented. It is obvious that CO exposure noticeably decreases the work function: it immediately

(59) Mugarza, A.; Mascaraque, A.; Repain, V.; Rousset, S.; Altmann, K. N.; Himpsel, F. J.; Koroteev, Y. M.; Chulkov, E. V.; García de Abajo, F. J.; Ortega, J. E. *Phys. Rev. B* **2002**, *66*, 245419.
(60) Hövel, H.; Barke, I. *Prog. Surf. Sci.* **2006**, *81*, 53–111.
(61) Michaelson, H. B. *J. Appl. Phys.* **1977**, *48*, 4729–4733.
(62) Mehmood, F.; Kara, A.; Rahman, T. S.; Henry, C. R. *Phys. Rev. B* **2009**, *79*, #075422.

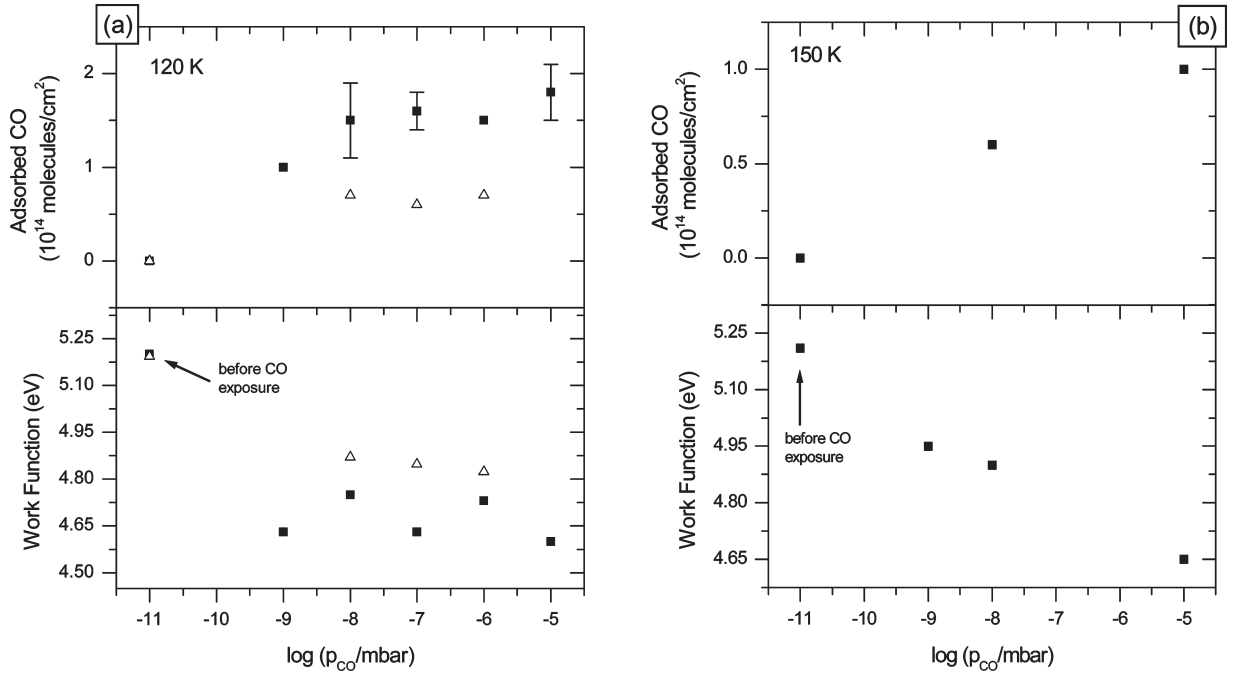

Figure 3. Variation of the amount of adsorbed CO and the work function of the sputter modified Au(111) surface as a function of the CO partial pressure. (a) Data measured at 120 K. (■) Sample roughened at 120 K and (Δ) sample roughened at 300 K and rapidly cooled to 120 K. (b) Data measured at 150 K (sample roughened at 120 K).

decreases by some 0.5 eV when the CO pressure rises in the chamber to above 10^{-9} mbar. Similarly to the adsorbed amount of CO, the work function change also saturates, indicating that the CO adsorbing capacity of the surface is limited.

Because of technical reasons, both the vibrational spectroscopic measurements and the STM experiments were carried out on samples roughened at room temperature, so it is worth discussing the effect of sample temperature during ion bombardment on the CO-related features of the UPS and XPS spectra. The valence band UPS spectra of the room temperature roughened samples (not shown here) exhibit very similar changes upon CO exposure at 120 K to those ion bombarded at low temperature. However, both the XPS analysis and the work function measurement reveal that room temperature roughening reduces the CO adsorbing capacity by approximately a factor of 2, most probably by annealing out a certain fraction of the CO binding sites (Figure 3a, open symbols). Further discussion of the effect of temperature on the CO adsorption process will be presented later in this work. Still, the important point is that there are qualitative similarities between CO adsorption on room temperature and 120 K roughened Au surfaces; therefore, the discussion of the adsorption in terms of the STM image presented in Figure 1 is feasible.

Recalling the analysis of the STM images, it turns out that the estimated density of step edge sites (2.4×10^{14} /cm^2) correlates very well with the amount of adsorbed CO (1×10^{14} to 2×10^{14} /cm^2). However, no other structural elements (kinks at step edge intersections, protrusions, etc.) exist at comparable density, showing that the step edge sites should be responsible for the adsorption of CO on the roughened surface. In fact, this conclusion gives a confirmation based on a quantitative argument of the adsorption mechanism proposed for similarly prepared samples in ref 35. Moreover, it is in very good agreement with the results of the qualitative evaluation of synchrotron-based high resolution photoemission data obtained on Au(310) and (312) surfaces.[27]

Temperature programmed desorption measurements on Au surfaces with (111) steps revealed a broad feature at around 130 K and a high temperature peak at around 170−180 K.[26,27] It was argued that although CO adsorbs on the step edge sites, the structure of the TPD curve may be due to substrate mediated long-range interactions between adsorbates.[27] Very similar TPD traces were recorded on ion bombardment modified surfaces.[35] These findings suggest that if the sample temperature is increased to above 130 K (i.e., the temperature of the first desorption maximum) then deviations from low temperature behavior (as discussed in connection with Figure 3a) can be anticipated. Indeed, as the data measured at 150 K (Figure 3b) show, the CO coverage becomes pressure dependent and does not reach saturation at up to 10^{-5} mbar. This information needs to be taken into consideration when discussing the sum frequency spectroscopy data, which were collected at 150 K.

In Figure 4a, the sum frequency spectra measured on sputter roughened Au(111) surfaces can be seen. One has to keep in mind during the interpretation of the results that the SFG spectrum of Au has an intense background (due to an electronic resonance according to the excitation of electrons from the d band to empty states above the Fermi level by the visible beam (2.33 eV)) and the SFG spectrum itself can be regarded as the interference pattern between the background and the vibrationally resonant features. In other words, the spectrum can be modeled by the following function

$$S(\omega_2) = \left| A_{\mathrm{NR}} e^{i\varphi_{\mathrm{NR}}} + \sum_m \frac{A_m e^{i\varphi_m}}{\omega_2 - \omega_m + i\Gamma_m} \right|^2 \qquad (1)$$

where $S(\omega_2)$ is the spectrum measured as the function of the frequency ω_2 of the infrared excitation, A_{NR} is the amplitude of the (vibrationally nonresonant) background, and A_m and Γ_m are the amplitude and width of the mth resonant mode.[63]

(63) Pászti, Z.; Wang, J.; Clarke, M. L.; Chen, Z. *J. Phys. Chem. B* **2004**, *108*, 7779–7787.

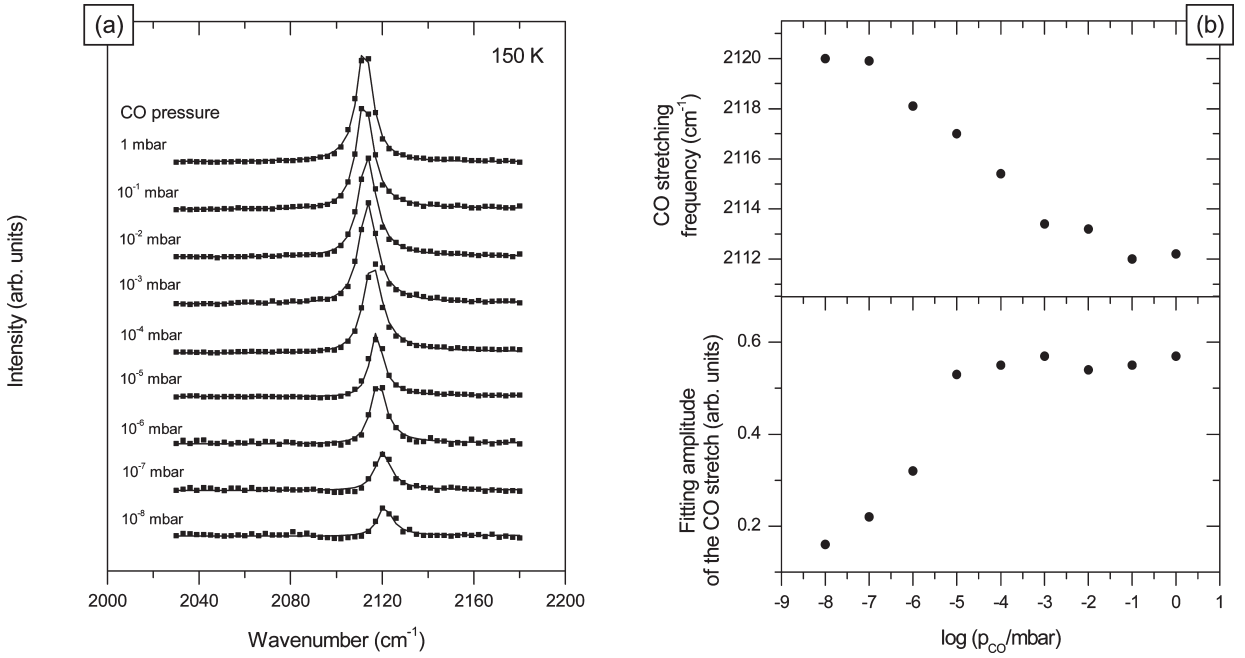

Figure 4. (a) Sum frequency spectra of the sputter modified Au(111) surface exposed to different CO partial pressures. Sputtering took place at room temperature, and CO adsorption experiments were carried out at 150 K. All spectra were taken in the ppp polarization combination. (b) Frequency of the CO vibration and amplitude of the resonant peak derived from fitting the spectra in panel (a), plotted as a function of the CO pressure.

The interference, due to the phase relation between the vibrational peak and the background, can cause significant alterations in the appearance of the spectrum if the phase is varied, even if the parameters of the resonant peak are kept constant.

Upon observation of the SFG spectra of CO on roughened Au(111) and their fitting according to the above equation (Figure 4), a strong feature can be seen at slightly above 2100 cm^{-1} at all studied pressures. This peak position was observed in numerous studies dealing with the infrared spectroscopic analysis of CO adsorption on gold surfaces[25,26,29,35,64,65] and can be assigned to CO molecules on top of gold atoms.

A more detailed inspection combined with spectral fitting reveals that all spectra can be quite well described by a single, narrow vibrational resonance (width parameter of around 4 cm^{-1}). In addition, the peak positions shift toward lower wavenumbers as the CO pressure is increased. Finally, the height of the vibrational features apparently increases with elevated gas pressure.

The fitting of our SFG spectra indicated that the decrease in the signal to below 10^{-5} mbar can indeed be traced to the decrease in the resonant fitting amplitude (Figure 4b), which correlates well with the observed pressure dependence of the amount of adsorbed CO at 150 K (Figure 3b). A simultaneous analysis of SFG spectra taken in the ppp polarization combination presented in Figure 4a and those measured in the ssp polarization combination (not shown) confirms that there is no major orientation change in the pressure range studied here, thus the fitting amplitude can be regarded as a direct measure of the amount of adsorbed CO. The SFG data therefore suggest that at this temperature the coverage saturates in slightly more than 10^{-5} mbar CO.

The shift of the CO vibrational frequency toward lower values as the CO coverage of the surface is increased is generally observed in UHV studies of CO interaction with Au single crystals of different orientations,[25,26,29] where CO exposures up to several Langmuirs are reported. Similar data were obtained by an infrared spectroscopic investigation of the adsorption of CO on sputter roughened Au(111),[35] also in the exposure range of a few Langmuirs. High-pressure experiments, usually carried out on supported gold catalysts at room temperature, also resulted in similar trends: an increase in CO pressure up to the 100 mbar range led to a decrease in the CO stretching frequency.[64,65]

Although commonly observed, the interpretation of the frequency shift is not straightforward. In certain cases, it was possible to deconvolute the measured spectra into contributions assigned to different adsorption sites,[25,64,66,67] while in other studies, in line with our own data, the CO vibrations were very sharp and shifted very smoothly, contradicting claims based on inhomogeneous broadening due to different adsorption sites.[26,35,65] As a result, an alternative explanation was offered for the negative shift of the CO vibrational frequency in terms of coverage-dependent changes in the extent of the CO−metal interaction (i.e., electron donation from 5σ orbitals to the metal), which competes with the dipole−dipole coupling among the CO adsorbates.[65]

To gain further insight into the bonding properties of CO on roughened Au(111), density functional calculations were carried out on surface models containing low-coordinated Au atoms. The following model geometries were studied: a smooth Au(111) surface with several fractional CO coverages ($^1/_{12}$ and $^1/_3$ monolayers), an Au adatom with CO (denoted as Au + CO), two Au adatoms with CO on each (2Au + 2CO), CO on a step edge modeled by an Au adatom triangle lying on the smooth surface (3Au + CO), the same structure with two CO adsorbates (3Au + 2CO), and CO interacting with a tetrahedron formed by a fourth Au atom added to the triangle (4Au + CO).

(64) Boccuzzi, F.; Tsubota, S.; Haruta, M. *J. Electron Spectrosc. Relat. Phenom.* **1993**, *64−65*, 241–250.
(65) France, J.; Hollins, P. *J. Electron Spectrosc. Relat. Phenom.* **1993**, *64−65*, 251–258.
(66) Brown, M. A.; Carrasco, E.; Sterrer, M.; Freund, H.-J. *J. Am. Chem. Soc.* **2010**, *132*, 4064–4064.
(67) Raskó, J.; Kiss, J. *Catal. Lett.* **2006**, *111*, 87–95.

Table 1. DFT Results for On-Top CO Adsorption on Different Sites of Au(111)-Based Surfaces

	ΔE(eV)	d_{Au-CO} Å	d_{CO} Å	ν_{CO} cm^{-1}
Au(111) + CO ($^1/_{12}$ ML)	0.26	2.04	1.148	2059
Au(111) + 4CO ($^1/_3$ ML)	0.18	2.05	1.150	2060
Au(111) + Au + CO	1.08	1.94	1.153	2066
Au(111) + 2Au + 2CO	1.1	1.96	1.154	2073
Au(111) + 3Au + CO	0.88	2.03	1.150	2059
Au(111) + 3Au + 2CO	0.86	2.04	1.151	2060
Au(111) + 4Au + CO	0.94	1.99	1.153	2072

The free CO molecule is characterized by the calculated stretching frequency of 2120 cm^{-1} at an equilibrated bond length of 1.146 Å. The corresponding experimental values are 2145 cm^{-1} and 1.128 Å.[68] Calculated adsorption energies and CO frequencies for the top site are presented in Table 1.

The data indicate little variation in the CO frequency and a very weak correlation between adsorption energy and frequency. The vibrational frequency correlates somewhat better with the coordination number of the adsorption site. Only a few computational studies on model gold surfaces have been performed. Using DFT calculations, several authors[28,62,69,70] showed that the stepped surface (Au(221), Au(331), and Au(8,7,4)) binds CO more strongly (0.6−1.0 eV) than the flat Au(111) surface (0.17−0.3 eV), similar to our findings.

The calculated data strongly suggest that the coverage dependent shift of the CO stretching frequency is due to the gradual population of the adsorption sites starting with those formed at very low coordinated Au atoms and proceeding toward those with higher coordination numbers.[25,64] Still, the lack of the appearance of different frequencies from inequivalent adsorption sites in the majority of the published infrared data is an issue requiring further analysis.

Our SFG results revealed exactly the same trends as observed for small exposures, although the spectra were measured under dynamic CO exposure conditions (i.e., the presence of gaseous CO allowed for establishing equilibrium between the gas and the adsorbate phases) and typically corresponded to CO doses of several hundreds or thousands of Langmuirs. This fact points to the importance of the adsorbed amount in determining the actual CO stretching frequency rather than to the role of other parameters such as temperature and pressure or the dose of CO exposure.

At the same time, our UPS measurements confirmed the presence of an electronic interaction between not only the gold d states but also the sp-originated confined surface state electrons and carbon monoxide adsorbates, indicating that electronic effects indeed may play a role in the change in the CO vibrational frequency. One may speculate that although it is still conceivable that the shift is due to the gradual filling of differently coordinated adsorption sites, strong coupling between the CO oscillators due to dipole−dipole interaction and/or effects mediated by the delocalized sp electrons of the substrate may smear out the small frequency differences between the adsorbates at structurally inequivalent sites, thus resulting in a single vibrational mode for the whole ensemble of adsorbed CO molecules.

Temperature Dependent Variations in the Adsorption of CO on Sputter Modified Au(111). In TPD experiments carried out on different Au surfaces, including those structured by ion bombardment, CO adsorbates completely desorbed at temperatures of around 190−200 K, which can therefore be regarded as the desorption temperature for traditional UHV surface science studies. Because to our knowledge no systematic investigation of the adsorption behavior of CO on Au single crystals was performed above this range, in the following paragraphs we will discuss our electron spectroscopic and vibrational data obtained during annealing the sample up to room temperature.

The temperature dependence of the CO adsorption properties was followed by photoelectron spectroscopy at pressures of 10^{-8} and 10^{-5} mbar. Figure 5 gives a summary of the temperature dependent changes in the adsorbed amount as determined from XPS measurements and in the work function derived from UPS spectra.

According to Figure 5a, there is no striking difference between the temperature dependence of the amount of adsorbed CO measured in a flow of gas with a pressure of 10^{-8} mbar and after a single CO dose at the same pressure. The amount of adsorbed CO continuously decreases with increasing temperature, and the work function increases to the value characteristic of the CO-free surface. From the work function data, one can deduce that the final desorption temperature is around 190 K, in very good agreement with the TPD results obtained on sputter roughened Au(111).[35] Although the trends are similar in 10^{-5} mbar CO (Figure 5b), the adsorbed amount data suggest and the work function values prove that whereas CO again desorbs at around 190 K in vacuum this pressure is high enough to maintain a small CO coverage up to at least 230−240 K.

A similar set of experiments concentrating on the temperature dependence of the vibrational features of the CO adsorbates was performed using SFG. Temperature dependent spectra taken in 10^{-8}, 10^{-5}, and 10^{-1} mbar CO are presented in Figure 6.

The SFG spectra taken in 10^{-8} and 10^{-5} mbar CO are in very good agreement with the electron spectroscopy data. In both cases, the signal gradually decreases, indicating the loss of CO adsorbates, and the desorption is complete by 200 K in the former case and by 230 K in the latter case, as already seen in the XPS and work function results (Figure 5). Spectra measured in 10^{-1} mbar CO give information from a pressure range not accessible to electron spectroscopy measurements. Again, a gradual decrease in the CO signal can be seen, although the desorption temperature increased to almost room temperature.

The frequency of the CO stretch changes only very slightly in 10^{-8} mbar CO during the temperature dependent experiment (from 2120 cm^{-1} at 150 K to 2122 cm^{-1} at 185 K), whereas in 10^{-5} mbar CO the shift is somewhat larger (from 2117 cm^{-1} at 150 K to 2121 cm^{-1} at 215 K). In 10^{-1} mbar CO, the CO frequency varies over an even broader range (from 2112 cm^{-1} at 150 K to 2119 cm^{-1} at 270 K). These tendencies confirm the relationship between the CO frequency and the adsorbed amount as suggested during the analysis of the pressure dependence of the CO adsorption at 150 K (Figure 4).

If CO is removed from the chamber after an exposure of several hundred Langmuirs at 150 K and the temperature dependence of the CO stretch is measured in vacuum, sum frequency spectra indicate a CO desorption temperature of around 180−190 K, independent of the pressure of the initial CO exposure. The desorption temperature derived from the SFG measurements for these low temperature CO adsorbates agrees nicely with that obtained from electron spectroscopy experiments.

The results presented in Figures 5 and 6 demonstrate that at temperatures lower than 190 K CO forms stable adsorbates on sputter roughened Au(111), as already pointed out by TPD measurements in ref 35. At higher temperatures, another CO

(68) Mantz, A. W.; Watson, J. K. G.; Rao, K. N.; Albritton, D. L.; Schmeltekope, A. L.; Zare, R. N. *J. Mol. Spectrosc.* **1971**, *39*, 180.
(69) Piccolo, L.; Loffreda, D.; Aires, F.; Deranlot, C.; Jugnet, Y.; Sautet, P.; Bertolini, J. C. *Surf. Sci.* **2004**, *566−568*, 995–1000.
(70) Liu, Z.-P.; Hu, P.; Alavi, A. *J. Am. Chem. Soc.* **2002**, *49*, 124.

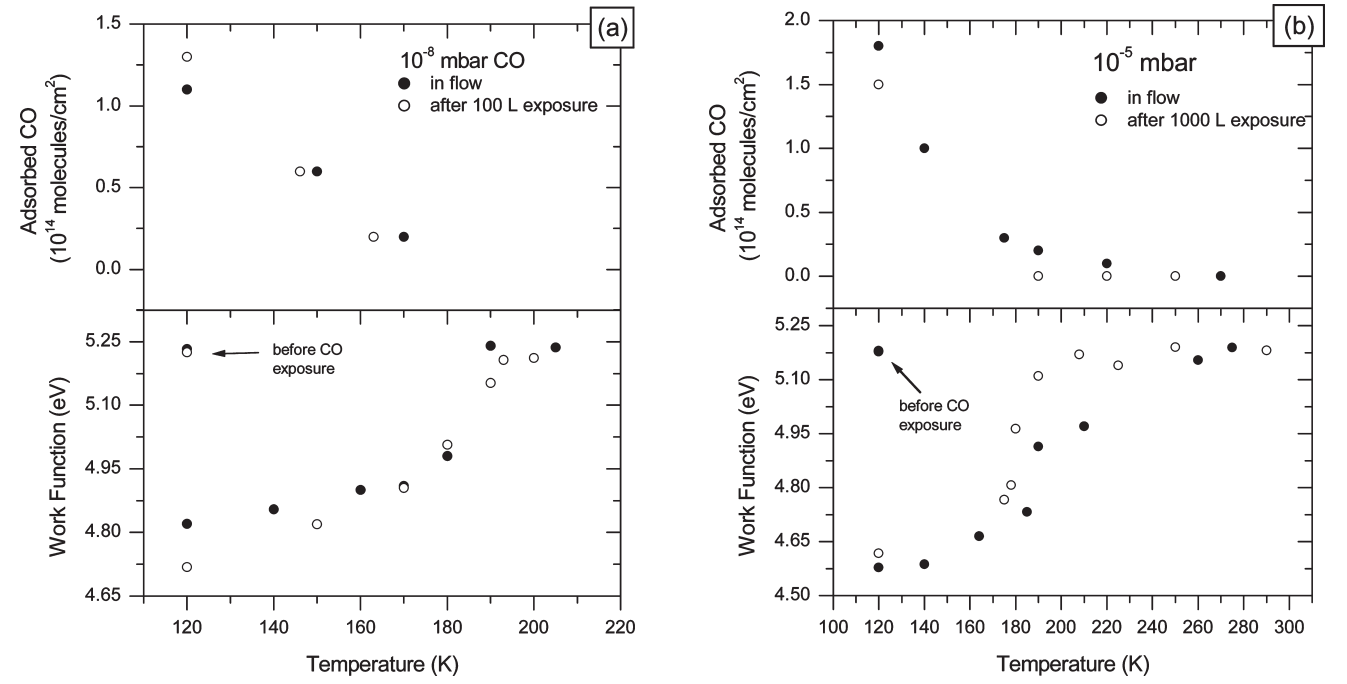

Figure 5. Changes in the amount of adsorbed CO (based on XPS data) and work function (from UPS) measured on ion bombardment modified Au(111) as a function of sample temperature. Sputtering and initial gas dosing were performed at 120 K in (a) 10^{-8} and (b) 10^{-5} mbar CO. (●) Data collected in CO and (○) data measured in vacuum after an initial CO exposure at the indicated pressure.

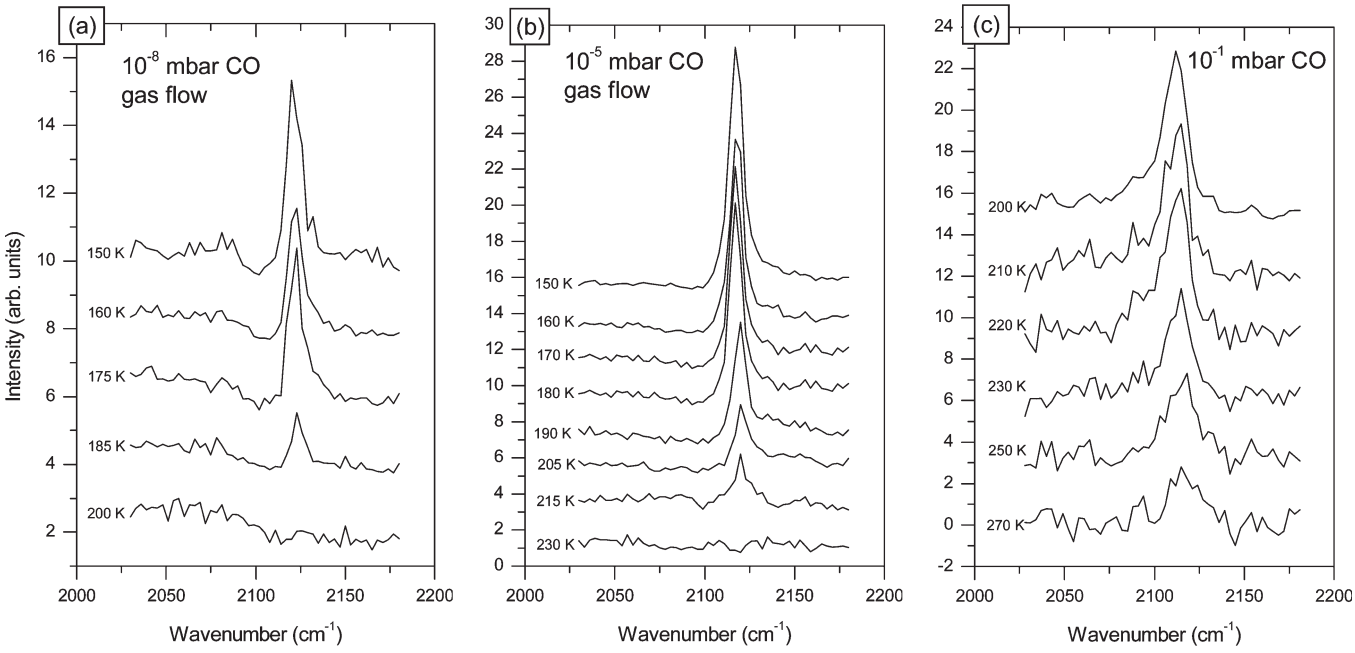

Figure 6. SFG spectra of CO adsorbates on ion bombardment modified Au(111) as a function of temperature. Spectra were taken in the ppp polarization combination. The Au(111) single crystal was roughened at room temperature and immediately placed on the cold sample holder of the SFG chamber. In (a) 10^{-8}, (b) 10^{-5}, and (c) 10^{-1} mbar CO.

adsorption regime exists in which adsorption can be detected only in the presence of gaseous CO, indicating the unstable nature of the adsorbates. In addition, the temperature of complete desorption depends on the CO pressure in this regime, approaching room temperature at 0.1 mbar. This observation correlates well with the appearance of CO adsorbates on Au(110) above 0.1 mbar at room temperature[71] or the detection of CO on supported Au nanoparticles upon exposure to several millibars of CO at room temperature.[64,65] In fact, we believe that because of the relationship between the CO pressure and the temperature of the complete desorption, the low pressure adsorbates found slightly above 200 K correspond in their nature to those appearing at room temperature in the millibar range, thus facilitating the modeling of the reactivity of Au in CO oxidation in systems accessible to traditional surface science tools.

(71) Jugnet, Y.; Cadete Santos Aires, F. J.; Deranlot, C.; Piccolo, L.; Bertolini, J. C. *Surf. Sci.* **2002**, *521*, L639–L644.

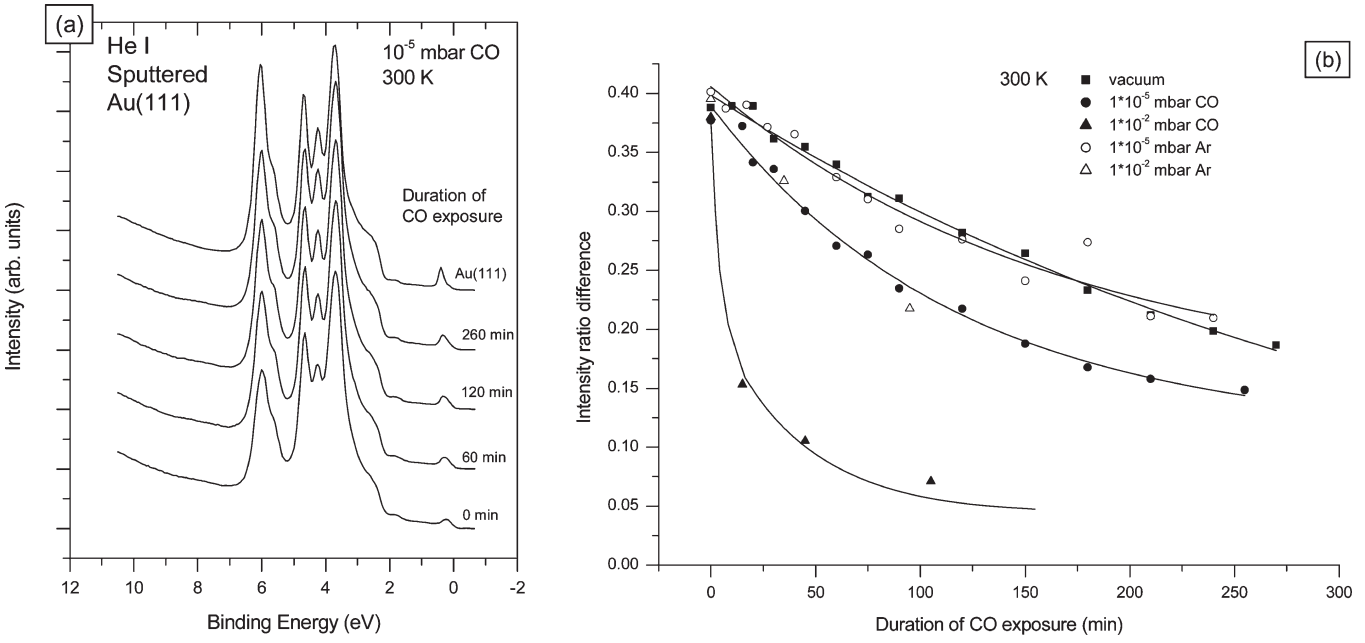

Figure 7. (a) Variation of the He I excited UPS spectrum of the sputter modified Au(111) surface during aging in 10^{-5} mbar CO at room temperature. For reference, the uppermost trace shows the room temperature spectrum of the intact Au(111) surface. (b) Variation of the difference in the height ratio of the 4.7/6.0 eV binding energy peaks of the He I excited UPS spectrum measured on the sputter modified and intact Au(111) surfaces as a function of aging time at room temperature in (■) vacuum, (●) 10^{-5} mbar CO, (▲) 10^{-2} mbar CO, (○) 10^{-5} mbar Ar and, (△) 10^{-2} mbar Ar.

CO-Assisted Rearrangement of the Roughened Au(111) Surface. A comparison of the UPS spectra of the sputter modified Au(111) surfaces taken before and after CO adsorption experiments, especially if annealing to room temperature at higher CO pressures was studied, revealed a striking change in the spectral features toward those of the unsputtered surface. Therefore, a separate set of experiments was designed to study the time dependent behavior of the surface and the CO adsorbates under various adsorption conditions. The results of these investigations are presented in the last subsection of our work.

In Figure 7a, as an example of the electronic structure changes found during annealing or aging the sample in CO, a set of He I excited valence band spectra are presented as a function of the time of CO exposure at room temperature. For comparison, the spectrum of the intact Au(111) surface is also shown.

Just after sputtering (0 min of CO exposure), the typical valence band spectrum of the roughened Au(111) appears. (See also Figure 4a.) As expected for this pressure−temperature combination, no obvious signs of CO adsorption can be noticed when the gas is admitted into the chamber. Instead, the surface state related structure starts to increase and shift toward higher binding energies, and the height ratio of the 4.7/6.0 eV binding energy d peaks begins to decrease, resulting in a valence band slowly approaching the shape of that of the intact surface as the exposure time proceeds. Because both mentioned spectral features are clearly structure sensitive as mentioned at the beginning of the Results and Discussion section, the observed electronic structure changes point to alterations in the short range atomic order toward that of the original Au(111) surface.

According to our experience, the difference between the height ratio of the 4.7/6.0 eV peaks measured on the sputter modified and intact Au(111) surfaces can serve as a sensitive probe of this reordering process. In Figure 7b, the time dependence of this quantity is presented for several gas pressures and compositions during room temperature experiments. Our experiments revealed that the reordering takes place also in the absence of carbon monoxide, although it is considerably slower than in 10^{-5} mbar CO. Argon exposure at 10^{-5} mbar has no effect on the process as the reordering kinetics are the same as in vacuum. In 10^{-2} mbar CO the structural change is particularly fast, while in 10^{-2} mbar Ar, the process is similar to what was seen in 10^{-5} mbar CO. Low temperature data, which were omitted from Figure 7b to

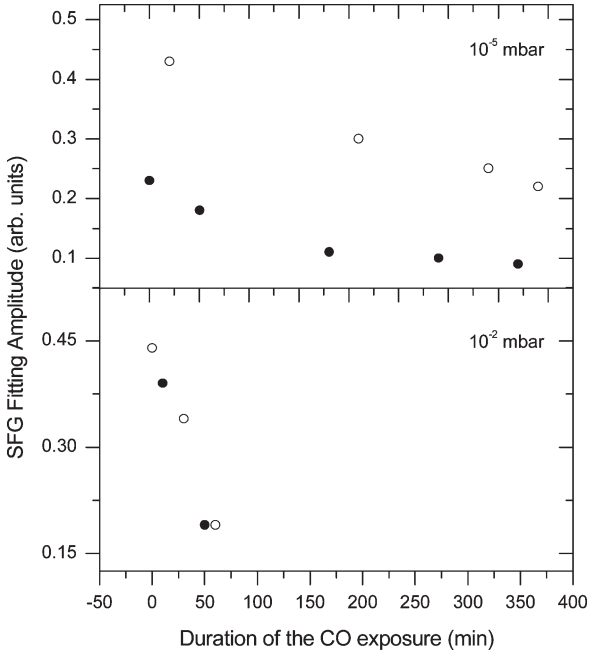

Figure 8. Exposition time dependence of the SFG fitting amplitude of the CO stretch measured on the sputtered Au(111) surface aged in 10^{-5} mbar CO (upper panel) and 10^{-2} mbar CO (lower panel). (●) Data measured at 210 K and (○) data measured after cooling the sample to 150 K in 10^{-5} mbar CO. Time was measured from the moment of CO admittance.

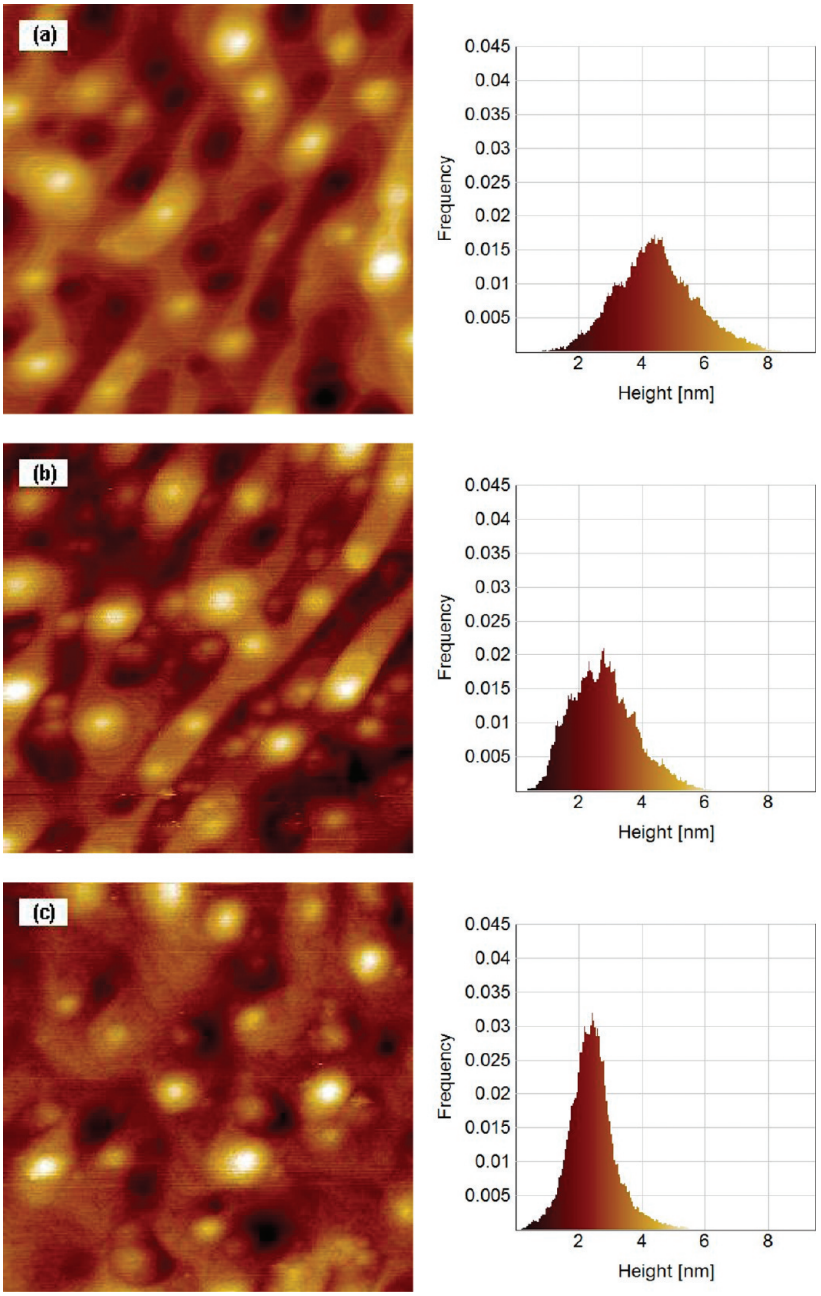

Figure 9. STM images (200×200 nm^2) of the sputter modified Au(111) surface (a) immediately after Ar^+ ion bombardment (10 min, 3 keV, 10 μA/cm^2 current density), (b) after 60 min of CO exposure at 10^{-4} mbar, and (c) after 60 min of CO exposure at 1 mbar. The z scale can be derived from the corrugation, which was (a) 8.6, (b) 6.8, and (c) 5.8 nm. Graphs on the right show the height distribution (measured from the lowest point) of the pixels of the images. All treatments and STM measurements were carried out at room temperature.

avoid overcrowding of the graph, show that at 120 K there are negligible time dependent changes in the UPS spectra either in the presence or in the absence of CO. At around 200 K, just above the desorption temperature of the stable CO adsorbates, the effect of CO on the reordering is still rather weak. These results suggest that the reordering is thermally activated, indicating that temperature dependent processes such as material transport by diffusion provide the kinetics leading to surface relaxation.

Because the ordered Au(111) surface does not adsorb a considerable amount of CO, one may guess that the CO binding capacity of the sputter modified surface decreases during reordering. In Figure 8, the time dependence of the SFG signal from CO adsorbates measured during aging at 10^{-5} and 10^{-2} mbar at around 210 K is compared. Because no signs of orientation change were observed (see above), the decrease in the fitting amplitude is due to the decrease in the amount of adsorbed CO. To separate the temperature dependence of the CO signal (as discussed previously) and the consequences of the decrease of the CO binding capacity due to reordering, fitting amplitudes derived from measurements at 210 K as well as data obtained after rapidly cooling the sample to 150 K are simultaneously presented. During quenching the sample was kept in 10^{-5} mbar CO, regardless of the pressure at which the 210 K data were measured.

In 10^{-5} mbar CO, the CO stretching amplitudes measured both at 210 K or after quenching to 150 K slowly decrease. Because the valence band UPS spectra recorded around 200 K showed few changes even during extended aging in CO, the first step in the

reordering must be the loss of the CO adsorption sites, which is a relatively slow process at 200−210 K. The SFG data correlate very well with those obtained by electron spectroscopy measurements in 10^{-5} mbar CO (Supporting Information). In 10^{-2} mbar CO, both amplitudes decrease much faster than those observed during aging in 10^{-5} mbar CO. This finding shows that reordering leading to the loss of CO binding sites becomes faster with increasing CO pressures even at this low temperature, by analogy to the results of the room temperature UPS experiments in Figure 7b.

Because spectroscopic investigations, whatever their sensitivity to local structural changes, provide only indirect evidence of surface reordering, STM measurements were also performed to clarify further the nature of the CO-induced relaxation of the sputter modified Au(111) surface. In Figure 9, the room temperature STM micrographs of the sample just after ion bombardment and after aging in CO are shown. To facilitate the comparison of the micrographs and visualize the evolution of the surface, histograms showing the height distribution of the images determined by the SPIP image processing software are also presented.

While the morphological elements of the sputtered surface (Figure 9a) are familiar from Figure 1b, CO exposure results in considerable smoothening, indicated by the narrowing of the height distribution curve as well as the decrease in the corrugation value from 8.6 to 6.8 nm after the 10^{-4} mbar CO exposure and 5.8 nm after the 1 mbar CO exposure. The density of the islandlike elements remained more or less constant, but the long, narrow terracelike structures connecting the islands started to disappear even in 10^{-4} mbar CO (Figure 9b), which continued until dispersed islands on a more or less structureless smooth surface were detected after the 1 mbar exposure (Figure 9c). Moreover, the pits so characteistic of the sputtered surface were also missing after the 1 mbar CO treatment. The analysis of the step edge atom density also showed a significant decrease from $2.4(\pm0.3) \times 10^{14}/\mathrm{cm}^2$ (for the just sputtered surface) to $1(\pm0.2) \times 10^{14}/\mathrm{cm}^2$ during the 1 mbar CO exposure. Meanwhile, a control experiment performed in vacuum indicated much smaller surface reordering even after 15 h of room temperature aging (image not shown).

Therefore, according to the presented data collected by surface spectroscopy as well as direct imaging techniques, the ion bombardment modified Au(111) surface is prone to spontaneous relaxation toward its originally smooth morphology even at temperatures near or somewhat below room temperature. This process is very significantly accelerated in the presence of carbon monoxide, especially if the CO pressure is relatively high. Remarkably, this reordering capability of CO remains pronounced even at temperatures where no CO adsorbates can be detected by surface spectroscopic tools. While the driving force of the relaxation can be traced to the highly nonequilibrium atomic distribution created by ion bombardment,[72,73] one may speculate that short-lived adsorbed CO species can in some way decrease the activation energy for surface diffusion involving material transport through step edges, leading to the massive reordering.

The CO facilitated reordering of the sputter modified Au(111) surface was found to eliminate the CO adsorption sites gradually. As a result, the temperature dependence of the CO adsorption as discussed previously is due to not only thermal desorption but also irreversible annealing out of certain CO binding sites.

In fact, CO-induced massive atomic movements were observed not only in a metastable system such as the sputter roughened Au(111) surface studied in this work. In ref 71, a structural and spectroscopic investigation of CO interaction with Au(110) at room temperature is presented. According to the results, at low CO pressure (from ultrahigh vacuum to 10^{-5} mbar) the surface exhibits (1×2) reconstruction, whereas in the millibar range this reconstruction becomes completely disrupted. Instead, the formation of monatomic-high islands can be seen, which assumes similar long range atomic movements as found in our study. In addition, surface X-ray diffraction experiments performed on Au(111) gave evidence for lifting of the $(22 \times \sqrt{3})$ reconstruction of the intact surface at CO pressures higher than 1 mbar,[74] although the nature and the extent of the structural changes are difficult to assess by the applied experimental technique. A spectroscopic investigation of CO adsorption and oxidation on Au nanoparticles supported by TiO_2 also pointed to the possibility of adsorbate-induced structural rearrangement of the particles.[67]

Because CO-facilitated reordering of Au surfaces seems not to be specific to a particular structure but occurs rather generally, we may speculate that supported nanoparticulate gold catalysts also undergo similar processes. In nanoparticles, the 3D particle geometry may hinder the development of a stable structure during CO exposure because low coordinated structures are continuously generated during reordering. Perhaps a mechanism like this CO-induced reordering can carry CO adsorbates from the nanoparticle itself to the particle−substrate boundary, where oxidation to CO_2 can proceed.

Conclusions

To obtain better insight into the interaction of carbon monoxide with gold catalysts, the CO adsorption properties of a model system based on an Au(111) single crystal surface modified by ion bombardment were investigated by photoelectron spectroscopy, sum frequency generation vibrational spectroscopy, and scanning tunneling microscopy at pressures ranging from ultrahigh vacuum to 1 mbar.

Spectroscopic data confirmed the formation of stable adsorbates on the roughened surface at low temperatures, which completely desorbed at around 190 K. An estimation of the amount of adsorbed CO from XPS data and statistics of the morphological elements created by sputtering derived from STM images revealed a very strong correlation between the surface density of the CO adsorbates and the number of Au atoms belonging to step edges, indicating that step edge sites are responsible for the CO binding capacity of the bombarded Au(111) surface. No CO adsorption was detected on the intact surface. Computational studies by density functional theory confirmed the role of the low coordinated Au atoms in CO adsorption and suggested a correlation between the coordination number of the binding site and the CO stretching frequency.

At sample temperatures above 200 K, unstable CO adsorbates were detected under dynamic CO exposure conditions, which disappeared immediately if gaseous CO was removed from the experimental chamber. A clear correlation was found between the CO pressure and the maximal temperature at which CO adsorbates can be found on the surface.

(72) Cheng, Y.-T. *Mater. Sci. Rep.* **1990**, *5*, 45–97.
(73) Kelly, R.; Miotello, A. *Nucl. Instrum. Methods Phys. Res., Sect. B* **1997**, *122*, 374–400.
(74) Peters, K. F.; Steadman, P.; Isern, H.; Alvarez, J.; Ferrer, S. *Surf. Sci.* **2000**, *467*, 10–22.

The ion bombardment roughened Au(111) surface was found to relax spontaneously toward the atomic order of the smooth surface even below room temperature. Our spectroscopic investigations provided evidence for the significant acceleration of this reordering in the presence of CO, which leads to the gradual elimination of the CO binding sites. A positive correlation was established between the reordering kinetics and the applied CO pressure. The STM investigations confirmed the occurrence of massive atomic movements facilitated by CO exposure.

Acknowledgment. The financial support of Hungarian Science and Research Fund OTKA (grant nos. NNF 78837, K69200, and K68052) is gratefully acknowledged.

Supporting Information Available: Details and discussion of the interaction of CO with the intact Au(111) surface, analysis of the XPS spectra of the CO adsorbates, and electron spectroscopy data on the aging of the roughened surface in 10^{-5} mbar CO at 210 K. This material is available free of charge via the Internet at http://pubs.acs.org.